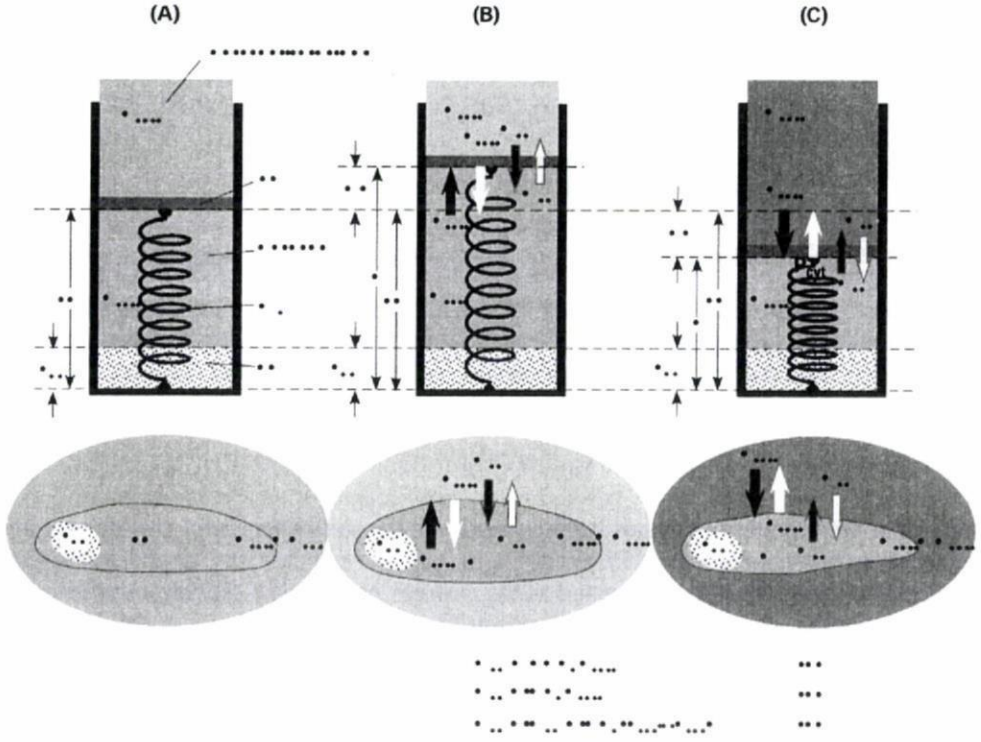


FIGURE 3.9 (See color insert following page 208.) Mechanoosmotic model of a Paramecium cell in an (A) isosmotic, (B) hypoosmotic, or (C) hyperosmotic solution. The model is drawn as a cylinder with a semipermeable piston (bar labeled SM) that is fixed to the bottom of the cylinder by a coil spring ($M_B$). The piston and the coil spring correspond to the semipermeable cell membrane and its elasticity (the bulk modulus of the cell), respectively. The inside and outside of the cylinder correspond to the cytosol and the external solution, respectively. Medium gray corresponds to the cytosolic osmolarity ($C_{cyt}$), lighter gray to an osmolarity of the external solution ($C_{ext}$) lower than $C_{cyt}$, and darker gray to a $C_{ext}$ higher than $C_{cyt}$. A dotted area in the cylinder corresponds to an osmotically nonactive portion of the cell (na). The corresponding cell shape is shown below each model. When $C_{ext} = C_{cyt}$ (A), no osmotic water flow takes place across the piston, so the coil spring is neither expanded nor compressed; that is, the cell is neither swollen nor shrunken. The length of the coil spring in this situation corresponds to its natural resting length. The corresponding cell volume is thereby termed the natural cell volume (vN). When $C_{ext}$ is lowered below $C_{cyt}$ (B), water osmotically flows into the cylinder through the piston (water inflow, $Q_{v\bullet}$; downward blue-bordered black arrow). $Q_{v\bullet}$ is proportional to the osmotic pressure of the cytosol with reference to the external solution so $\bullet_{cyt}$ (upward black arrow) can be obtained from Equation 1, where A is the area of the semipermeable cell membrane and $L_p$ is the hydraulic conductivity of the membrane. A hydrostatic pressure in the cytosol with reference to the external solution $P_{cyt}$ (downward white arrow) is generated as the coil spring is expanded by the water inflow (the cell is osmotically swollen) and causes a water outflow from the cylinder through the piston (upward blue-bordered white arrow labeled $Q_{vP}$), which is proportional to $P_{cyt}$ (Equation 2). $Q_{vP}$ cancels $Q_{v\bullet}$ and the overall water flow across the piston becomes 0 when the cell swells to a level where $P_{cyt} = \bullet_{cyt}$ and, therefore, $Q_{vP} = Q_{v\bullet}$ (Equation 3). Inversely, when $C_{ext}$ is raised beyond $C_{cyt}$ (C), the water osmotically leaves the cylinder through the piston (the water outflow; upward blue-bordered black arrow labeled $Q_{v\bullet}$), so the coil spring is compressed (the cell is osmotically shrunken)• A negative hydrostatic pressure with reference to the external solution is thereby generated in the cylinder and causes a water inflow through the piston (downward blue-bordered white arrow labeled $Q_{vP}$). The overall water flow across the piston becomes 0 when the coil spring is compressed to a level where $P_{cyt} = \bullet_{cyt}$ and, therefore, $Q_{vP} = Q_{v\bullet}$ (Equation 3). For discussion see Baumgarten and Feher.[11] Abbreviations: $v_{na}$, volume of the osmotically nonactive portion of the cell (na); v, cell volume; • v, volume change after changing the external osmolarity.

where $v_{na}$ is the volume of the osmotically nonactive portion (nonaqueous phase) of the cell (Figure 3.9). For each $C_{adp}$ range ($C_{adp} < 75$, $75 < C_{adp} < 160$, or $160 < C_{adp} < 245$ mmol/L), N can be written as:

$$N \cdot C_N \cdot v_N \cdot v_{na} \cdot \quad (3.5)$$

because $C_{cyt} = C_N$ and $v = v_N$, when $C_{adp} = C_N$.

The values for $C_{cyt_n}$, $\cdot_{cyt_n}$, and $M_{B_n}$ can be estimated from the data in Figure 3.10A and Figure 3.8A according to Equations 3.1 to 3.5 based on the assumption that $v_{na}$ remains constant in the specific $C_{adp}$ range employed, as represented in Figure 3.8 (B, $C_{cyt_n}$; C, $\cdot_{cyt_n}$; D, $M_{B_n}$). The value for $v_{na}$ is not available at present so we employed two different plausible values for $v_{na}$: 20 and 40% of the cell volume of cells growing in the original culture medium (84 mOsmol/L) for the estimation (black and gray lines in Figure 3.8B, C, and D correspond to 20 and 40%, respectively). Changes in these parameters caused by a change in $C_{adp}$ are essentially the same for the two different $v_{na}$ cases; that is, $\cdot_{cyt}$ is highest (greater than ~1.6 • $10^5$ Pa) at its lower $C_{adp}$ values in each range, where the difference between $C_{cyt}$ and $C_{adp}$ is largest, and it is almost 0 at the highest $C_{adp}$ values because, at these values, their difference is essentially 0 (Equation 3.1).

That the cell volume decreases continuously as the adaptation osmolarity increases (Figure 3.8A), even though the cytosolic osmolarity increases stepwise (Figure 3.8B), implies that the resistance by the cell to volume change (its $M_B$) also increases stepwise at each critical osmolarity as $C_{adp}$ increases. $M_B$ is highest at the highest $C_{adp}$ values in each osmolarity range, and the highest value in each $C_{adp}$ range is larger in the higher osmolarity range (~12, ~17, and ~114 • $10^5$ Pa at 75, 160, and 245 mOsmol/L for $C_{adp}$, respectively). For an easier understanding of the mechanoosmotic behaviors of a Paramecium cell, a cell model is presented in Figure 3.9 that is consistent with the mechanoosmotic behaviors exhibited by the cell when the external osmolarity is changed.

## B. Regulatory Volume Control

### 1. Time Course of Change in Cell Volume after Changing the External Osmolarity

When a cell adapted to a specific $C_{adp}$ is transferred into another solution with an osmolarity ($C_{stm}$) different from the $C_{adp}$, the $\cdot_{cyt}$ changes so the cell volume will change until a new balance for $\cdot_{cyt}$ and $P_{cyt}$ is established (Equations 3.1 and 3.2). The time courses for the changes in volume of 16 groups of cells adapted to different $C_{adp}$ after they were each transferred into a different stimulatory $C_{stm}$ are shown in Figure 3.10. $C_{adp}$ and $C_{stm}$ for each group are visualized by vertical arrows in each corresponding inset. Downward and upward arrows correspond to a decrease and an increase, respectively, in the external osmolarity upon subjection of a cell to the stimulatory $C_{stm}$. The number at the tail end of each arrow indicates the $C_{adp}$ and the number at the head end indicates $C_{stm}$ in mOsmol/L. The length of each arrow corresponds to the amount of change in the external osmolarity upon subjecting the cell to $C_{stm}$ (black, gray, and light gray arrows correspond to 60, 40, and 20 mOsmol/L of change, respectively). A horizontal bar that crosses an arrow corresponds to a $C_N$ (75 or 160 mOsmol/L) and is placed on the same osmolarity scale with that for the arrows. When the arrow crosses a horizontal bar, the external osmolarity is changed beyond a $C_N$ (Figure 3.10A, C, D, F, H, I); when the arrow does not cross a horizontal bar, the external osmolarity is changed in an osmolarity range where no $C_N$ is crossed (Figure 3.10B, E, G, J). Some representative microscope images of the cells adapted to different $C_{adp}$ before and 15 and 30 min after subjecting the cell to a different $C_{stm}$ are shown in Figure 3.11.

### 2. Activation of RVD

When the external osmolarity is decreased ($C_{stm} < C_{adp}$; see Figure 3.10A–E, downward arrows), cell volume increases with time to a higher level (osmotic swelling). The cell volume then resumes its initial level only if the osmolarity decrease crosses a $C_N$ (Figure 3.10A, C, D; see also Figure

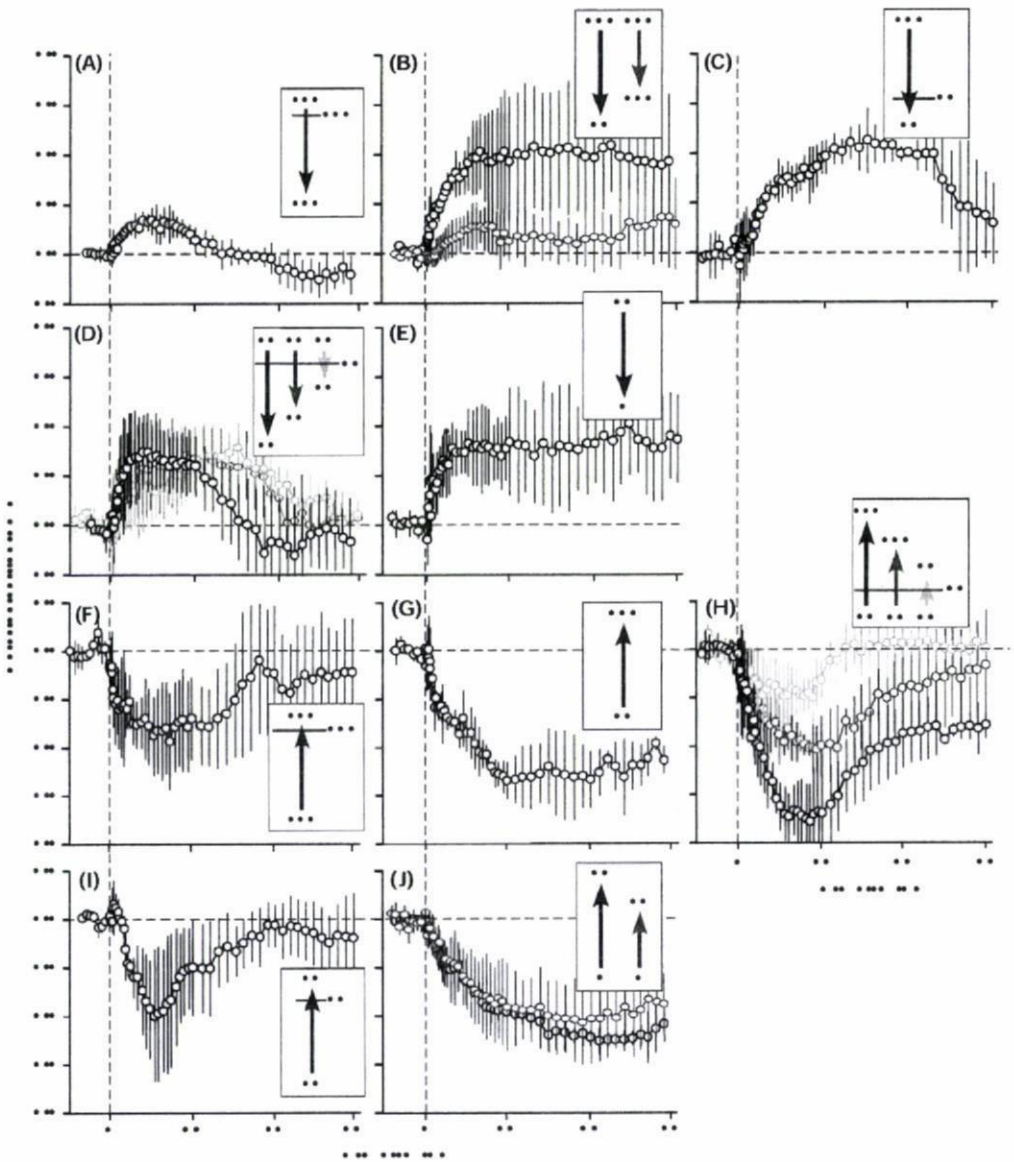


FIGURE 3.10 Time courses of change in cell volume after decreasing (A–E) or increasing (F–J) the external osmolarity in 16 different groups of Paramecium multimicronucleatum. Black, gray, and light gray circles correspond to changes in the external osmolarity by 60, 40, and 20 mOsmol/L, respectively. Arrows in the insets show (1) the direction of the osmolarity change (i.e., downward corresponds to its decrease and upward to its increase), and (2) the degree of change in the osmolarity (i.e., the long black, medium gray, and short light gray arrows correspond to 60, 40, and 20 mOsmol/L changes, respectively). The number at the tail end is the adaptation osmolarity ($C_{adp}$), and that at the head end is the changed osmolarity ($C_{stm}$) in mOsmol/L. A horizontal bar across the arrow corresponds to a critical osmolarity ($C_N$), where the change in osmolarity has crossed a $C_N$. The value for the $C_N$ is shown as a number beside the bar. See the text for details. (Adapted from Iwamoto, M. et al., J. Exp. Biol., 208, 523, 2005. With permission.)

3.11B). By contrast, the cell volume stays at the higher level if no $C_N$ is crossed (Figure 3.10B, E; see also Figure 3.11A). These findings imply that an outward-directed osmolyte-transport mechanism that decreases $C_{cyt}$ (with subsequent cell volume decreases) is activated when $C_{stm}$ is decreased

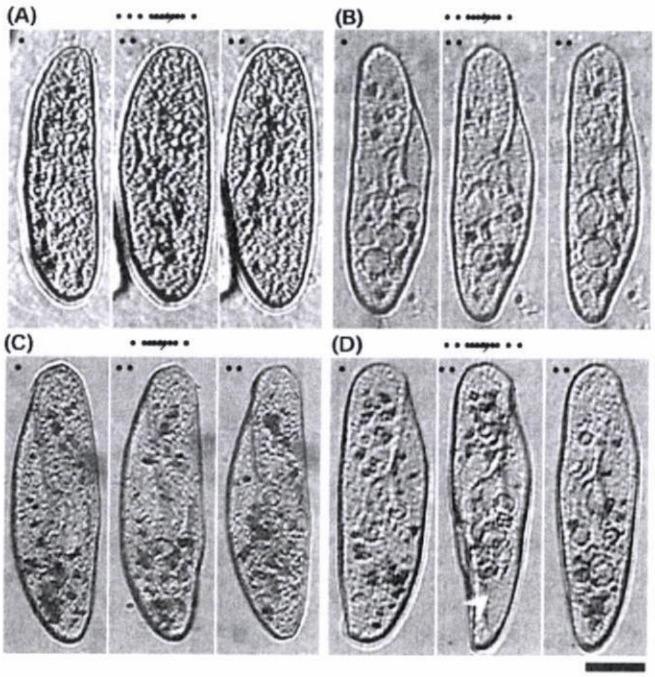


FIGURE 3.11 Four sets of three consecutive pictures of a representative cell each obtained from a different group of Paramecium multimicronucleatum cells adapted to one of four different osmolarities taken at 0, 15, and 30 min, respectively, after changing the external osmolarity by 60 mOsmol/L. (A) A 144-mOsmol/L-adapted cell was subjected to 84 mOsmol/L. (B) A 84-mOsmol/L-adapted cell was subjected to 24 mOsmol/L. (C) A 4-mOsmol/L-adapted cell was subjected to 64 mOsmol/L. (D) A 64-mOsmol/L-adapted cell was subjected to 124 mOsmol/L. A white arrowhead points to an indentation of the cell caused by osmotic shrinkage of the cell. The top of each cell image corresponds to the anterior end of the cell. A number on the upper left corner of each picture is the time in minutes, after changing the external osmolarity, when the picture was taken. Scale bar, 50 • m. (From Iwamoto, M. et al., J. Exp. Biol., 208, 523, 2005. With permission.)

beyond a $C_N$. This osmolyte-transport mechanism corresponds to a regulatory volume decrease (RVD) mechanism (see Chapter 2).

It is clear from the figures that the following are not directly correlated with the activation of RVD: (1) the amount of decrease in the external osmolarity, represented as the length of a downward arrow; (2) the maximum amount of swelling of the cell, represented as a peak or plateau value for cell volume; and (3) the rate of increase in cell volume, which corresponds to the tangent to the time course of cell volume change after decreasing the external osmolarity.

As is shown in Figure 3.8C, $P_{cyt}$ of an adapted cell is highest when $C_{adp}$ is lowest—that is, close to $C_N$ in a given $C_{adp}$ range (as at ~75 in the $C_{adp}$ < 75 mOsmol/L range or ~160 in the 160 < $C_{adp}$ < 245 mOsmol/L range), as the cell is maximally swollen at this $C_{adp}$ value (Figure 3.8A). If a cell adapted to an osmolarity in one of the above $C_{adp}$ ranges is subjected to an external osmolarity lower than the $C_N$ at the lower end of the range, the cell would be expected to swell more than the maximal value observed and $P_{cyt}$ should increase beyond the highest value obtained. In contrast, however, $P_{cyt}$ does not exceed the highest value when the adapted cell is subjected to an osmolarity increase within the specific $C_{adp}$ range. It is therefore concluded that an increase in $P_{cyt}$ beyond the highest value is a primary factor required for activation of RVD.

Currently, we do not know how an increase in $P_{cyt}$ beyond the highest value (the threshold value) will cause RVD to be activated. There might be a pressure sensor or a tension sensor in the cell membrane that is triggered by osmotic swelling of the cell that may, in turn, activate the RVD system to release osmolytes from the cell across its membrane.

The threshold $P_{cyt}$ is approximately1.5 to 1.9 • $10^5$ Pa (Figure 3.8C). The threshold membrane tension estimated from the $P_{cyt}$ value approximates 2 N/m, which is thousands of times larger than the threshold tension required for activation of some mechanosensitive ion channels.[40,81] This high pressure must be countered by the expansion of a cytoskeletal system that lines the plasma membrane or the cell pellicle, which has a high bulk modulus. The tension in the plasma membrane, where the hypothetical RVD mechanism is thought to reside, when expanded to the same degree as the cytoskeleton, would appear to be much lower than that of the estimated tension in the cytoskeletal lining.

### 3. Activation of RVI

When the external osmolarity is increased ($C_{stm} > C_{adp}$; Figure 3.10F–J, upward arrows), the cell volume decreases with time to a lower value. It then resumes its initial value when the osmolarity increases beyond a $C_N$ (Figure 3.10F, H, I; see also Figure 3.11D). In contrast, cell volume remains at the lower value when the increase in external osmolarity occurs within a range where no $C_N$ is crossed (Figure 3.10G, J; see also Figure 3.11C). These findings imply that an inward-directed osmolyte-transport mechanism that increases $C_{cyt}$ (cell volume consequently increases) is activated when $C_{stm}$ is increased beyond a $C_N$. This osmolyte-transport mechanism corresponds to a regulatory volume increase (RVI) mechanism. As is similar to the case for RVD, the amount of increase in the external osmolarity (the length of the upward arrows), the maximum amount of decrease in cell volume (the lower peak or plateau value for cell volume), and the rate of decrease in cell volume (the tangent to the time course of cell volume change) after increasing the external osmolarity are not directly correlated with the activation of RVI.

As shown in Figure 3.8C, $P_{cyt}$ of an adapted cell is almost 0 when $C_{adp}$ is highest in a specific $C_{adp}$ range where no $C_N$ is included (as at ~75 in the $C_{adp}$ < 75 mOsmol/L range or ~160 in the 75 < $C_{adp}$ < 160 mOsmol/L range), as the cell is neither swollen nor shrunken at a $C_{adp}$ that is close to $C_N$. If a cell adapted to a given osmolarity is subjected to an external osmolarity higher than $C_N$ at the border of this $C_{adp}$ range that includes the given osmolarity, $P_{cyt}$ should become negative and the cell would shrink. Because $P_{cyt}$ never becomes negative when the external osmolarity is increased within the given osmolarity range, it is therefore concluded that a decrease to 0 or a negative $P_{cyt}$ is the primary factor required for activation of RVI. The cell shrinks and the cell membrane wrinkles when $P_{cyt}$ becomes 0 (Figure 3.11D, white arrowhead). A 0 or negative pressure sensor or a wrinkle-sensitive mechanosensor must be involved in the activation of RVI.

### 4. Regulatory Volume Control Involves $K^+$ Channels of the Cell Membrane

When a stimulatory solution contains 10 mmol/L tetraethylammonium (TEA) (a potent $K^+$ channel inhibitor), adapted cells that would normally be stimulated to undergo RVD or RVI are not so stimulated. In these cells, the volume increases (upon decreasing the external osmolarity) or decreases (upon increasing the external osmolarity) to a new plateau level without returning to their initial volumes. In the presence of 30 mmol/L of $K^+$, RVD is also inhibited so the cell volume increases without showing a resumption of the initial volume after decreasing the external osmolarity to a point that RVD should have been activated. On the other hand, RVI is enhanced so cell volume is restored more quickly then normal after increasing the external osmolarity to a point where RVI would normally be activated.[54] These findings strongly suggest that $K^+$ channels in the plasma membrane of the cell are involved in regulatory volume control mechanisms in Paramecium in both RVD and RVI. Involvement of several kinds of $K^+$ channels in regulatory cell volume control has been demonstrated in several cell types.[11,48,81,89] (Also refer to Chapter 2.)

## C. Cell Volume Control and CVC Activity

Four representative time courses of change in the CVC activity presented as $R_{CVC}$ after changing the external osmolarity by 60 mOsmol/L are shown in Figure 3.12. In Figure 3.12A, a 164-mOsmol/L-adapted cell was subjected to 104 mOsmol/L; the external osmolarity was decreased beyond a $C_N$

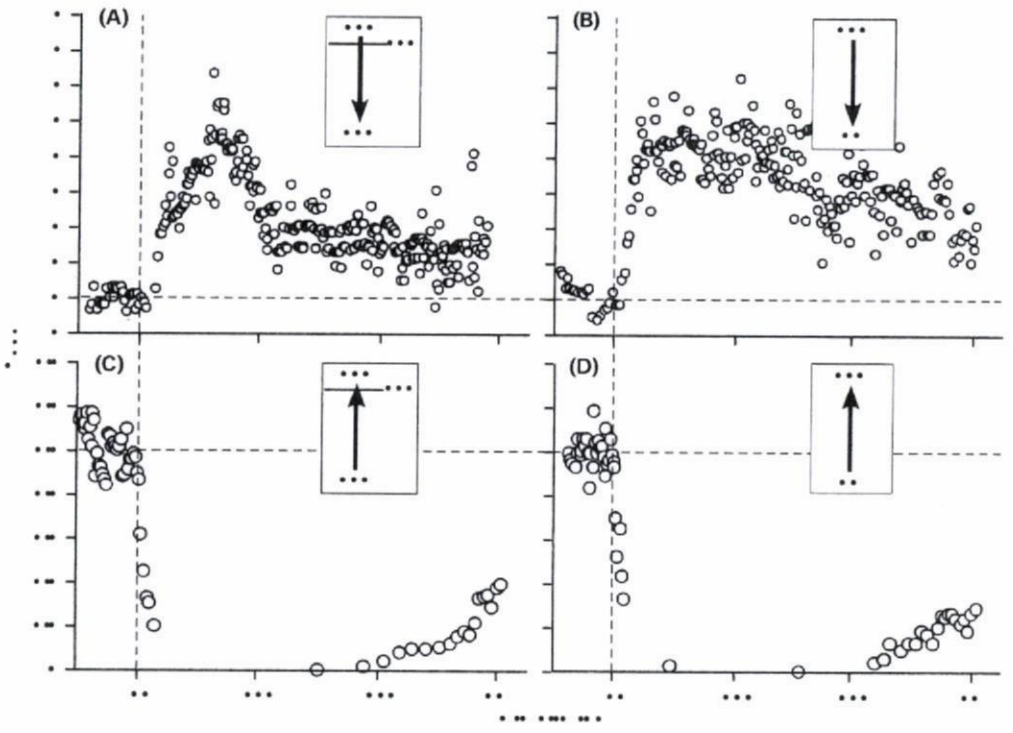


FIGURE 3.12 Four representative time courses of change in the rate of fluid segregation and discharge by the contractile vacuole ($R_{CVC}$) after changing the external osmolarity by 60 mOsmol/L in Paramecium multimicronucleatum. (A) A 164-mOsmol/L-adapted cell was subjected to 104 mOsmol/L. (B) A-144 mOsmol/L-adapted cell was subjected to 84 mOsmol/L. (C) A 104-mOsmol/L-adapted cell was subjected to 164 mOsmol/L. (D) A 84-mOsmol/L-adapted cell was subjected to 144 mOsmol/L. An arrow in each inset shows the direction of change in the external osmolarity; the downward arrow (A, B) corresponds to a decrease, while the upward arrow (C, D) to an increase. A number at the tail end shows the adaptation osmolarity and that at the head end shows the changed external osmolarity in mOsmol/L. A horizontal bar that crosses the arrow corresponds to a $C_N$, indicating that the change in the external osmolarity crossed a $C_N$. A number beside the bar is the osmolarity of the $C_N$. (From Iwamoto, M. et al., J. Exp. Biol., 208, 523, 2005. With permission.)

of 160 mOsmol/L so RVD was activated and the cell volume returned to normal. The corresponding time course of change in cell volume is shown in Figure 3.10A. In Figure 3.12B, a 144-mOsmol/L-adapted cell was subjected to 84 mOsmol/L; the osmolarity change was made without crossing a $C_N$ so RVD was not activated and the cell volume remained higher than normal. The corresponding time course of change in cell volume is shown in Figure 3.10B. In Figure 3.12C, a 104-mOsmol/L-adapted cell was subjected to 164 mOsmol/L; the external osmolarity was changed beyond a $C_N$ of 160 mOsmol/L so RVI was activated and the cell volume approached a normal value. The corresponding time course of change in cell volume is shown in Figure 3.10F. In Figure 3.12D, an 84-mOsmol/L-adapted cell was subjected to 144 mOsmol/L; the osmolarity change was made without crossing a $C_N$ so RVI was not activated and cell volume remained below normal. The corresponding time course of change in cell volume is shown in Figure 3.10G.

In the cases of osmolarity decrease, $R_{CVC}$ appeared to increase in parallel with an increase in cell volume; that is, $R_{CVC}$ increased as cell volume increased after subjection of the cell to a 60-mOsmol/L decrease in the external osmolarity. $R_{CVC}$ then decreased when the cell volume resumed its initial value after activation of RVD (compare Figure 3.12A with Figure 3.10A), while $R_{CVC}$ remained higher when the RVD was not activated; therefore, the cell volume also remained higher (compare Figure 3.12B with Figure 3.10B).

$C_{cyt}$ decreases as the cell osmotically swells. The reduction of $C_{cyt}$, therefore, appears to be involved in enhancing the $R_{CVC}$ activity. It is highly probable that control by the cell of the ratio of osmolarity in the CV fluid ($C_{CVC}$) to cytosolic osmolarity ($C_{CVC}/C_{cyt}$) is a primary factor for determining the $R_{CVC}$ activity. When the ratio increases over the ratio existing before changing the external osmolarity, $R_{CVC}$ will become higher. When the cell resumes its initial volume after activation of RVD (Figure 3.10A), $C_{cyt}$ is assumed to decrease to the same extent as the decrease in external osmolarity. We previously reported that the ionic activities of the $K^+$ and $Cl^-$ ions in the CV fluid are reduced stepwise similar to the overall cytosolic osmolarity that follows RDV activation.[110] Thus, the CV fluid is also affected by RDV activation, and the cell keeps its ratios of $K^+$ and $Cl^-$ activities in the CVC to those in the $C_{cyt}$ more or less constant at ~2.4 (Table 3.1).[110] $R_{CVC}$, therefore resumes its previous value as the cell volume resumes its initial value (Figure 3.12A). Quantitative analysis of the relationship between the $C_{CVC}/C_{cyt}$ ratio and $R_{CVC}$ is necessary to understand the control mechanism of the rate of water segregation by the CVC ($R_{CVC}$).

On the other hand, the time course of change in $R_{CVC}$ after increasing the external osmolarity by 60 mOsmol/L was essentially the same, independently of whether RVI was activated or not (compare Figure 3.12C and D with Figure 3.10F and G, respectively), That is, $R_{CVC}$ became 0 immediately after the cell was subjected to an increase in the external osmolarity. It began to recover around 30 to 40 min after increasing the external osmolarity and then gradually increased with time. These findings imply that a decrease in cell volume or a concomitant increase in $C_{cyt}$ or a decrease in $C_{CVC}/C_{cyt}$, caused by an increase in the external osmolarity, is not directly correlated with the inhibition of $R_{CVC}$. In fact, as explained earlier, we have determined that the decorated tubules, which bear the electrogenic V-ATPases, immunologically disappear when the cell is subjected to increases in external osmolarity, and it takes 60 to 120 min for the CVC membrane potential to return again to its plateau value of +80 mV.[39] $R_{CVC}$ cannot return to normal until the decorated tubules with their V-ATPases are reattached to the CVC.

It is unlikely that the CVC of Paramecium regulates the overall cell volume during either RVD or RVI by extrusion of cytosolic water and osmolytes through the CV. The initial rapid increase in $R_{CVC}$ when the cell is subjected to a decreased external osmolarity will buffer the cell against mechanical disruption that could result from a large initial osmotic swelling. Similarly, the rapid decrease in $R_{CVC}$ to 0 upon subjecting the cell to an increased external osmolarity would eliminate the effects of continued CVC activity upon the cell if excessive osmotic shrinkage were to occur. Dunham and his colleagues[31,112] had earlier suggested a role for the CV in buffering the osmotic changes in cell volume.

## D. Parasitic Protozoa

Physiological responses to hypoosmotic stress have been studied in parasitic protozoa, such as Trypanosoma,[101] Giardia,[91] Crithidia,[16] and Leishmania.[122] These parasitic protozoa encounter a wide range of fluctuation in external osmolarity as they progress through their life cycles; that is, a single life cycle that begins in the gut of the intermediate host (insects) may end in the cytoplasm of the definitive host (mammals). Docampo and his collaborators[101] demonstrated that Trypanosoma cruzi showed RVD in response to hypoosmotic stress in their various life-cycle stages. The major osmolytes responsible for RVD are neutral and anionic amino acids instead of $K^+$ and $Cl^-$, which are the predominant osmolytes responsible for RVD in many cell types, including Paramecium.[11,48,65,89,110] The efflux is assumed to be mediated by some putative osmotic swelling-sensitive organic anion channels.[58,59] They also demonstrated that external $Ca^{2+}$ ions were indispensable for triggering RVD in T. cruzi. It is generally accepted in many cell types that external $Ca^{2+}$ ions that enter the cytosol through osmotic swelling-sensitive $Ca^{2+}$ channels in the plasma membrane are the mediators of RVD.[65,123] Interestingly, control of the cytosolic $Ca^{2+}$ concentration by using $Ca^{2+}$ ionophores showed little effects on the amino acid efflux responsible for RVD. They concluded that, although $Ca^{2+}$ appears to play a role in modulating the early phase of amino acid efflux, it is not a key determinant of the final outcome of RVD.

## IV. FUTURE WORK ON PROTOZOAN OSMOREGULATION AND VOLUME CONTROL

One of the most pressing questions waiting to be answered in CVC research is the osmolarity of the CV in protozoa other than Paramecium. Most Dictyostelium researchers seem to have accepted the unproven conclusion that the CV of this cell is hypoosmotic to the cytosol.[46,107] This must be confirmed or disproved using in situ techniques that can be applied to the living cells of these small protozoa. In addition, the ion channels and osmolyte transport systems of the plasma membrane and CVC membranes must be explored with regard to their possible osmoregulatory and water and osmolyte secretion activities: biochemically, molecularly, and proteomically. Finally, as with the osmolarity of the CV, the number of organisms investigated must be increased to look for differences in the CVC cycle that may be revealed in different species.

Physiological studies on the regulatory volume control in Paramecium have only just begun; therefore, various conventional physiological approaches are now required to compare physiological characteristics of this specific cell with other cells for which more detailed physiological studies have already been completed. The comparison will potentially lead to a better understanding of physiological mechanisms underlying cell volume control. Some suggested experiments include the following: (1) Continuous measurement of the cellular membrane potential after changing the external osmolarity would reveal the dynamic change in the cytosolic $K^+$ concentration associated with RVD or RVI, as the resting membrane potential of Paramecium is dependent predominantly on $K^+$.[83] (2) Continuous monitoring electrically with a $Ca^{2+}$-sensitive microelectrode[110] or photometrically using a $Ca^{2+}$-sensitive dye of the cytosolic $Ca^{2+}$ concentration after changing the external osmolarity would reveal the possible involvement of $Ca^{2+}$ in modulating RVD or RVI. (3) Examination of the effects of appropriate channel inhibitors on the time course of cell volume change would reveal the ion channels that directly or indirectly participate in RVD or RVI.

To characterize RVD or RVI, simultaneous monitoring of associated cellular events such as changes in cell volume, cytosolic osmolarity, membrane potential, cytosolic activities of $K^+$ and $Cl^-$, etc. are indispensable. We are developing a novel intracellular osmometer.[82] The tip of the probe of the osmometer is ~2 • m in diameter so it can be inserted into the cell together with other microelectrodes for measuring membrane potential and ion activity. The basic principles of the microcapillary osmometer are illustrated in Figure 3.13. At present, the semipermeable $Cu_2Fe(CN)_6$ plug at the tip of the probe is too short lived (~3 min) to be very useful. Development of a long-lasting (at least 1 hr) semipermeable plug is necessary for the practical use of this technique.

The probe without a semipermeable plug can be used for monitoring the change in the hydrostatic pressure of the cytosol after changing the external osmolarity. Measurements of the cytosolic pressure are indispensable for estimation of the volume of the osmotically nonactive portion of the cytoplasm as well as the bulk modulus of the cell.

## REFERENCES

1. Akbarieh, M. and Couillard, P., Ultrastructure of the contractile vacuole and its periphery in Amoeba proteus: evolution of vesicles during the cycle, J. Protozool., 35, 99–108, 1988.
2. Allen, R.D., Membrane tubulation and proton pumps, Protoplasma, 189, I–8; 1995.
3. Allen, R.D., The contractile vacuole and its membrane dynamics, BioEssays, 22,1035–1042, 2000.
4. Allen, R.D. and Fok, A.K., Membrane dynamics of the contractile vacuole complex of Paramecium, J. Protozool., 35, 63–71, 1988.
5. Allen, R.D. and Fok, A.K., Membrane trafficking and processing in Paramecium, Int. Rev. Cytol., 198, 277–318, 2000.
6. Allen, R.D. and Naitoh, Y., Osmoregulation and contractile vacuoles of protozoa. In Molecular Mechanisms of Water Transport Across Biological Membranes, Zeuthen, T. and Stein, W.D., Eds., Academic Press, New York (reviewed in Int. Rev. Cytol., 215, 351–394, 2002).

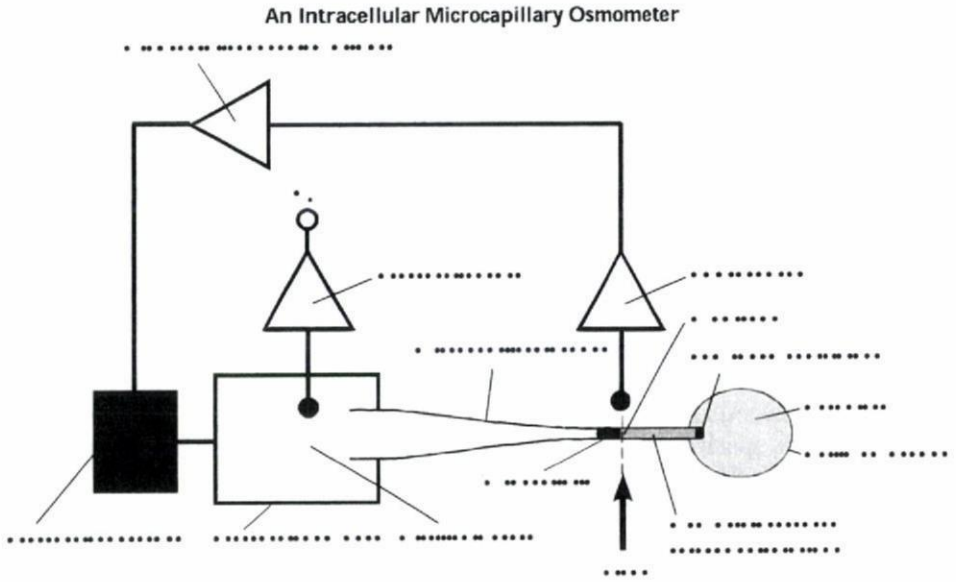


FIGURE 3.13 A novel intracellular microcapillary osmometer that can measure the osmolarity of the cytosol with a time constant of less than 1 sec. The microcapillary probe (the tip of a glass microcapillary similar in shape and dimensions to a conventional glass microcapillary electrode) is first plugged by a semipermeable material such as cupric ferrocyanide. An osmotic pressure reference solution is then introduced into the capillary and mineral oil is introduced to make a meniscus between the reference solution and the mineral oil in the capillary. When the tip of the probe is inserted into a cell, water moves across the plug according to an osmotic pressure difference between the reference solution and the cytosol, causing the meniscus to shift. The shift of the meniscus is detected by a photosensor that produces an electric signal proportional to the shift. The electric signal is amplified and fed into a pressure generator to generate a counter hydrostatic pressure in the pressure chamber to which the probe is connected and prevent a shift of the meniscus. The counter pressure required to prevent a shift in the meniscus is monitored by using a pressure sensor in the pressure chamber. The output of the sensor ($V_P$) corresponds to the counter pressure. The difference between the counter pressure and the osmotic pressure of the reference solution is the osmotic pressure of the cytosol.

7. Allen, R.D. and Wolf, R.W., Membrane recycling at the cytoproct of Tetrahymena, J. Cell Sci., 35, 217–227, 1978.
8. Allen, R.D., Ueno, M.S., Pollard, L.W., and Fok A.K., Monoclonal antibody study of the decorated spongiome of contractile vacuole complexes of Paramecium, J. Cell Sci., 96, 469–475, 1990.
9. Almsherqi, Z.A., Kohlwein, S.D., and Deng, Y., Cubic membranes: a legend beyond the Flatland of cell membrane organization, J. Cell Biol., 173, 839–844, 2006.
10. Andrus, W. de W. and Giese, A.C., Mechanisms of sodium and potassium regulation in Tetrahymena pyriformis W., J. Cell. Comp. Physiol., 61, 17–30, 1963.
11. Baumgarten, C. M. and Feher, J. J., Osmosis and regulation of cell volume. In Cell Physiology Source Book, 3rd ed., Sperelakis, N., Ed., Academic Press, San Diego, CA, 2001, pp. 319–355.
12. Becker, M., Matzner, M., and Gerisch, G., Drainin required for membrane fusion of the contractile vacuole in Dictyostelium is the prototype of a protein family also represented in man, EMBO J., 18, 3305–3316, 1999.
13. Beitz, E., Aquaporins from pathogenic protozoan parasites: structure, function and potential for chemotherapy, Biol. Cell, 97, 373–383, 2005.
14. Betapudi, V., Mason, C., Licate, L., and Egelhoff, T.T., Identification and characterization of a novel • -kinase with a von Willebrand factor A-like motif localized to the contractile vacuole and Golgi complex in Dictyostelium discoideum, Mol. Biol. Cell, 16, 2248–2262, 2005.

15. Brauer, E.B. and McKanna, J.A., Contractile vacuoles in cells of a fresh water sponge, Spongilla lacustris, Cell Tissue Res., 192, 309–317, 1978.
16. Bursell, J. D. H., Kirk, J., Hall, S. T., Gero, A. M., and Kirk, K., Volume-regulatory amino acid release from the protozoan parasite Crithidia luciliae, J. Membr. Biol., 154, 131–141, 1996.
17. Bush, J., Temesvari, L., Rodriguez-Paris, J., Buczynski, G., and Cardelli, J., A role for a Rab4-like GTPase in endocytosis and in regulation of contractile vacuole structure and function in Dictyostelium discoideum, Mol. Biol. Cell, 7, 1623–1638, 1996.
18. Chapman, G.B. and Kern, R.C., Ultrastructural aspects of the somatic cortex and contractile vacuole of the ciliate, Ichthyophthirius multifiliis Fouquet, J. Protozool., 30, 481–490, 1983.
19. Clark, T.B., Comparative morphology of four genera of trypanosomatidae, J. Protozool., 6, 227–232, 1959.
20. Clarke, M. and Heuser, J., Water and ion transport. In Dictyostelium: A Model System for Cell and Developmental Biology, Maeda, Y., Inouye, K., and Takeuchi, I., Eds., University Academic Press, Tokyo, 1997, pp. 75–91.
21. Clarke, M. and Maddera, L., Distribution of alkaline phosphatase in vegetative Dictyostelium cells in relation to the contractile vacuole complex, Eur. J. Cell Biol., 83, 289–296, 2004.
22. Clarke, M., Köhler, J., Arana, Q., Liu, T., Heuser, J., and Gerisch, G., Dynamics of the vacuolar $H^+$-ATPase in the contractile vacuole complex and the endosomal pathway of Dictyostelium cells, J. Cell Sci., 115, 2893–2905, 2002.
23. Couillard, P., Forget, J., and Pothier, F., The contractile vacuole of Amoeba proteus. III. Vacuolar response to phagocytosis. J. Protozool., 32, 333–338, 1985.
24. Cronkite, D.L. and Pierce, S.K., Free amino acids and cell volume regulation in the euryhaline ciliate Paramecium calkinsi, J. Exp. Zool., 251, 275–284, 1989.
25. Damer, C.K., Bayeva, M., Hahn, E.S., Rivera, J., and Socec, C.I., Copine A, a calcium-dependent membrane-binding protein, transiently localizes to the plasma membrane and intracellular vacuoles in Dictyostelium, BMC Cell Biol., 6, 46, 2005.
26. De Lozanne, A., The role of BEACH proteins in Dictyostelium, Traffic, 4, 6–12, 2003.
27. Doberstein, S.K., Baines, I.C., Wiegand, G., Korn, E.D., and Pollard, T.D., Inhibition of contractile vacuole function in vivo by antibodies against myosin-I, Nature, 365, 841–843, 1993.
28. Docampo, R., de Souza, W., Miranda, K., Rohloff, P., and Moreno, S.N.J., Acidocalcisomes: conserved from bacteria to man, Nature Rev. Microbiol., 3, 251–261, 2005.
29. Docampo, R., Scott, D.A., Vercesi, A.E., and Moreno, S.N.J., Intracellular $Ca^{++}$ storage in acidocalcisomes of Trypanosoma cruzi, Biochem. J., 310, 1005–1012, 1995.
30. Dunham, P.B. and Child, F.M., Ion regulation in Tetrahymena, Biol. Bull., 121, 129–140, 1961.
31. Dunham, P.B. and Kropp, D.L., Regulation of solutes and water in Tetrahymena. In Biology of Tetrahymena, Elliott, A.M., Ed., Dowden, Hutchinson and Ross, Stroudsburg, PA, 1973, pp. 165–198.
32. Fok, A.K., Aihara, M.S., Ishida, M., Nolta, K.V., Steck, T.L., and Allen, R.D., The pegs on the decorated tubules of the contractile vacuole complex of Paramecium are proton pumps, J. Cell Sci., 108, 3163–3170, 1995.
33. Fok, A.K., Clarke, M., Ma, L., and Allen, R.D., Vacuolar $H^+$-ATPase of Dictyostelium discoideum: a monoclonal antibody study, J. Cell Sci., 106, 1103–1113, 1993.
34. Fok, A.K., Yamauchi, K., Ishihara, A., Aihara, M.S., Ishida, M., and Allen, R.D., The vacuolar-ATPase of Paramecium multimicronucleatum: gene structure of the B subunit and the dynamics of the V-ATPase-rich osmoregulatory membranes, J. Eukaryot. Microbiol., 49, 185–196, 2002.
35. Furukawa, R. and Fechheimer, M., Differential localization of • -actinin and the 30 kD actin-bundling protein in the cleavage furrow, phagocytic cup and contractile vacuole of Dictyostelium discoideum, Cell Motil. Cytoskel., 29, 46–56, 1994.
36. Gabriel, D., Hacker, U., Köhler, J., Müller-Taubenberger, A., Schwartz, J.-M., Westphal, M., and Gerisch, G., The contractile vacuole network of Dictyostelium as a distinct organelle: its dynamics visualized by a GFP marker protein, J. Cell Sci., 112, 3995–4005, 1999.
37. Gerald, N.J., Siano, M., and De Lozanne, A., The Dictyostelium LvsA protein is localized on the contractile vacuole and is required for osmoregulation, Traffic, 3, 50–60, 2002.
38. Gerisch, G., Heuser, J., and Clarke, M., Tubular-vesicular transformation in the contractile vacuole system of Dictyostelium, Cell Biol. Int., 26, 845–852, 2002.

39. Grønlien, H.K., Stock, C., Aihara, M.S., Allen, R.D., and Naitoh, Y., Relationship between the membrane potential of the contractile vacuole complex and its osmoregulatory activity in Paramecium multimicronucleatum, J. Exp. Biol., 205, 3261–3270, 2002.
40. Gustin, M. C., Mechanosensitive ion channels in yeast: mechanism of activation and adaptation. Adv. Compar. Environ. Physiol., 10, 19–38, 1992.
41. Harris, E., Yoshida, K., Cardelli, J., and Bush, J., A Rab11-like GTPase associates with and regulates the structure and function of the contractile vacuole system in Dictyostelium, J. Cell Sci., 114, 3035–3045, 2001.
42. Hauser, K., Pavlovic, N., Kissmehl, R., and Plattner, H., Molecular characterization of a sarco(endo)plasmic reticulum ATPase gene from Paramecium tetraurelia and localization of this gene product to subplasmalemmal calcium stores. Biochem. J., 334, 31–38, 1998.
43. Hausmann, K. and Allen, R.D., 1977. Membranes and microtubules of the excretory apparatus of Paramecium caudatum, Cytobiologie (Eur. J. Cell Biol.), 15, 303–320, 1977.
44. Hausmann, K. and Patterson, D.J., Involvement of smooth and coated vesicles in the function of the contractile vacuole complex of some cryptophycean flagellates, Exp. Cell Res., 135, 449–453, 1981.
45. Hausmann, K. and Patterson, D.J., Contractile vacuole complexes in algae. In Compartments in Algal Cells and Their Interaction, Wiessner, W., Robinson, D., and Starr, R.C., Eds., Springer-Verlag, Berlin, 1984, pp. 139–146.
46. Heuser, J., Evidence for recycling of contractile vacuole membrane during osmoregulation in Dictyostelium amoebae: a tribute to Günther Gerisch, Eur. J. Cell Biol., 85, 859–871, 2006.
47. Heuser, J., Zhu, Q., and Clarke, M., Proton pumps populate the contractile vacuoles of Dictyostelium amoebae, J. Cell Biol., 121, 1311–1327, 1993.
48. Hoffman, E.K. and Dunham, P.B., Membrane mechanisms and intracellular signaling in cell volume regulation, Int. Rev. Cytol., 161, 173–262, 1995.
49. Hohmann, S., Osmotic adaptation in yeast: control of the yeast osmolyte system, Int. Rev. Cytol., 215, 149–187, 2002.
50. Ishida, M., Aihara, M.S., Allen, R.D., and Fok, A.K., 1993, Osmoregulation in Paramecium: the locus of fluid segregation in the contractile vacuole complex, J. Cell Sci., 106, 693–702, 1993.
51. Ishida, M., Aihara, M.S., Allen, R.D., and Fok, A.K., Acidification of the young phagosomes of Paramecium is mediated by proton pumps derived from the acidosomes, Protoplasma, 196, 12–20, 1997.
52. Ishida, M., Fok, A.K., Aihara, M.S., and Allen, R.D., Hyperosmotic stress leads to reversible dissociation of the proton pump-bearing tubules from the contractile vacuole complex in Paramecium, J. Cell Sci., 109, 229–237, 1996.
53. Iwamoto, M., Allen, R.D., and Naitoh, Y., Hypo-osmotic or $Ca^{2+}$-rich external conditions trigger extra contractile vacuole complex generation in Paramecium multimicronucleatum, J. Exp. Biol., 206, 4467–4473, 2003.
54. Iwamoto, M., Sugino, K., Allen, R.D., and Naitoh, Y., Cell volume control in Paramecium: factors that activate the control mechanisms, J. Exp. Biol., 208, 523–537, 2005.
55. Kaneshiro, E.S., Dunham, P.B., and Holtz, G.G., Osmoregulation in a marine ciliate, Miamiensis avidus. I. Regulation of inorganic ions and water, Biol. Bull., 136, 63–75, 1969.
56. Kaneshiro, E.S., Holtz, G.G., and Dunham, P.B., Osmoregulation in a marine ciliate, Miamiensis avidus. II. Regulation of intracellular free amino acids, Biol. Bull., 137, 161–169, 1969.
57. King, R.L., The contractile vacuole of Paramecium multimicronucleata, J. Morph., 58, 555–571, 1935.
58. Kirk, K. Swelling-activated organic osmolyte channels, J. Membr. Biol., 158, 1–16, 1997.
59. Kirk, K. and Strange, K., Functional properties and physiological roles of organic solute channels, Annu. Rev. Physiol., 60, 719–739, 1998.
60. Kissmehl, R., Froissard, M., Plattner, H., Momayezi, M., and Cohen, J., NSF regulates membrane traffic along multiple pathways in Paramecium, J. Cell Sci., 115, 3935–3946, 2002.
61. Kissmehl, R, Schilde, C., Wassmer, T., Danzer, C., Nuehse, K., Lutter, K., and Plattner, H., Molecular identification of 26 syntaxin genes and their assignment to the different trafficking pathways in Paramecium, Traffic, 8, 523–542, 2007.
62. Kitching, J.A., Contractile vacuoles, ionic regulation and excretion. In Research in Protozoology, Vol. 1, Chen, T.-T., Ed., Pergamon Press, Oxford, 1967, pp. 305–336.

63. Klein, R.L., Effects of active transport inhibitors on K movements in Acanthamoeba sp., Exp. Cell Res., 34, 231–238, 1964.
64. Knetsch, M.L.W., Schäfers, N., Horstmann, H., and Manstein, D.J., The Dictyostelium Bcr/Abr-related protein DRG regulates both Rac- and Rab-dependent pathways, EMBO J., 20, 1620–1629, 2001.
65. Lang. F., Bush, G.L., and Volk, H., The diversity of volume regulatory mechanisms, Cell. Physiol. Biochem., 8, 1–45, 1998.
66. Lefkir, Y., de Chassey, B., Dubois, A., Bogdanovic, A., Brady, R.J., Destaing, O., Bruckert, F., O'Halloran, T.J., Cosson, P., and Letourneur, F., The AP-1 clathrin-adaptor is required for lysosomal enzymes sorting and biogenesis of the contractile vacuole complex in Dictyostelium cells, Mol. Biol. Cell, 14, 1835–1851, 2003.
67. Linder, J.C. and Staehelin, L.A., A novel model for fluid secretion by the trypanosomatid contractile vacuole apparatus, J. Cell Biol., 83, 371–382, 1979.
68. Liu, T. and Clarke, M., The vacuolar proton pump of Dictyostelium discoideum: molecular cloning and analysis of the 100 kDa subunit, J. Cell Sci., 109, 1041–1051, 1996.
69. Luykx, R., Hoppenrath, M., and Robinson, D.G., Structure and behavior of contractile vacuoles in Chlamydomonas reinhardtii, Protoplasma, 198, 73–84, 1997.
70. Lynn, D.H., Dimensionality and contractile vacuole function in ciliated protozoa, J. Exp. Zool., 223, 219–229, 1982.
71. Marchesini, N., Ruiz, F.A., Vieira, M., and Docampo, R., Acidocalcisomes are functionally linked to the contractile vacuole of Dictyostelium discoideum, J. Biol. Chem., 277, 8146–8153, 2002.
72. McKanna, J.A., Fine structure of the contractile vacuole pore in Paramecium, J. Protozool., 20, 631–638, 1973.
73. McKanna, J.A., Permeability modulating membrane coats. I. Fine structure of fluid segregation organelles of peritrich contractile vacuoles, J. Cell Biol., 63, 317–322, 1974.
74. McKanna, J.A., Fine structure of the fluid segregation organelles of Paramecium contractile vacuoles, J. Ultrastruct. Res., 54, 1–10, 1976.
75. Miranda, K., Benchimol, M., Docampo, R., and de Souza, W., The fine structure of acidocalcisomes in Trypanosoma cruzi, Parasitol. Res., 86, 373–384, 2000.
76. Mitchell, H.J. and Hardham, A.R., Characterisation of the water expulsion vacuole in Phytophthora nicotianae zoospores, Protoplasma, 206, 118–130, 1999.
77. Moniakis, J., Coukell, M.B., and Forer, A., Molecular cloning of an intracellular P-type ATPase from Dictyostelium that is up-regulated in calcium-adapted cells, J. Biol. Chem., 270, 28276–28281, 1995.
78. Moniakis, J., Coukell, M.B., and Janiec, A., Involvement of the $Ca^{2+}$-ATPase PAT1 and the contractile vacuole in calcium regulation in Dictyostelium discoideum, J. Cell Sci., 112, 405–414, 1999.
79. Montalvetti, A., Rohloff, P., and Docampo, R., A functional aquaporin co-localizes with the vacuolar proton pyrophosphatase to acidocalcisomes and the contractile vacuole complex of Trypanosoma cruzi, J. Biol. Chem., 279, 38673–38682, 2004.
80. Morgan, A. and Burgoyne, R.D., Is NSF a fusion protein? Trends Cell Biol., 5, 335–339, 1995.
81. Morris, E., Mechanosensitive ion channels in eukaryotic cells. In Cell Physiology Source Book, 3rd ed., Sperelakis, N., Ed., Academic Press, San Diego, CA, 2001, pp. 745–760.
82. Naitoh, Y., Real time measurement of the osmolarities of the cytosol and the contractile vacuole fluid in Paramecium by using a microcapillary osmometer, Mol. Biol. Cell, 13(Suppl.), 223a, 2002.
83. Naitoh, Y. and Eckert, R., Electrical properties of Paramecium caudatum: modification by bound and free cations, Z. vergl. Physiol., 61, 427–452, 1968.
84. Naitoh, Y., Tominaga, T., Ishida, M., Fok, A.K., Aihara, M.S., and Allen, R.D., How does the contractile vacuole of Paramecium expel fluid? Modelling the expulsion mechanism, J. Exp. Biol., 200, 713–721, 1997.
85. Naitoh, Y., Tominaga, T., and Allen, R.D., The contractile vacuole fluid discharge rate is determined by the vacuole size immediately before the start of discharge in Paramecium multimicronucleatum, J. Exp. Biol., 200, 1737–1744, 1997.
86. Nishihara, E., Shimmen, T., and Sonobe, S., Functional characterization of contractile vacuole isolated from Amoeba proteus, Cell Struct. Funct., 29, 85–90, 2004.
87. Nolta, K.V. and Steck, T.L., Isolation and initial characterization of the bipartite contractile vacuole complex from Dictyostelium discoideum, J. Biol. Chem., 269, 2225–2233, 1994.

88. O'Halloran, T.J. and Anderson, R.G.W., Clathrin heavy chain is required for pinocytosis, the presence of large vacuoles, and development in Dictyostelium, J. Cell Biol., 118, 1371–1377, 1992.
89. O'Neil, W. C., Physiological significance of volume regulatory transporters, Am. J. Physiol., 276, C995–C1011, 1999.
90. Pao, G.M., Wu, L.-F., Johnson, K.D., Höfte, H., Chrispeels, M.J., Sweet, G., Sandal, N.N., and Saier, Jr., M.H., Evolution of the MIP family of integral membrane transport proteins, Mol. Microbiol., 5, 33–37, 1991.
91. Park, J.H., Schofield, P.J., and Edwards, M.R., The role of alanine in the acute response of Giardia intestinalis to hypo-osmotic shock, Microbiology, 141, 2455–2462, 1995.
92. Patterson, D.J., Contractile vacuoles and associated structures: their organization and function, Biol. Rev., 55, 1–46, 1980.
93. Plattner, H., Habermann, A., Kissmehl, R., Klauke, N., Majoul, I., and Söling, H.-D., Differential distribution of calcium stores in Paramecium cells: occurrence of a subplasmalemmal store with a calsequestrin-like protein, Eur. J. Cell Biol., 72, 297–306, 1997.
94. Prusch, R.D., Protozoan osmotic and ionic regulation. In Transport of Ions and Water in Animals, Gupta, B.L., Moreton, R.B., and Oschman, J.L., Eds., Academic Press, London, 1977, chap. 14.
95. Prusch, R.D. and Dunham, P.B., Contraction of isolated contractile vacuoles from Amoeba proteus, J. Cell Biol., 46, 431–434, 1970.
96. Prusch, R.D. and Dunham, P.B., Ionic distribution in Amoeba proteus, J. Exp. Biol., 56, 551–563, 1972.
97. Quiviger, B., de Chastellier, C., and Ryter, A., Cytochemical demonstration of alkaline phosphatase in the contractile vacuole of Dictyostelium discoideum, J. Ultrastruct. Res., 62, 228–236, 1978.
98. Riddick, D.H., Contractile vacuole in the amoeba Pelomyxa carolinensis, Am. J. Physiol., 215, 736–740, 1968.
99. Rivero, F., Illenberger, D., Somesh, B.P., Dislich, H., Adam, N., and Meyer, A.-K., Defects in cytokinesis, actin reorganization and the contractile vacuole in cells deficient in RhoGDI, EMBO J., 21, 4539–4549, 2002.
100. Rohloff, P., Montalvetti, A., and Docampo, R., Acidocalcisomes and the contractile vacuole complex are involved in osmoregulation in Trypanosoma cruzi, J. Biol. Chem., 279. 52270–52281, 2004.
101. Rohloff, P., Rodrigues, C.O., and Docampo, R., Regulatory volume decrease in Trypanosoma cruzi involves amino acid efflux and changes in intracellular calcium, Mol. Biochem. Parasitol., 126, 219–230, 2003.
102. Ruiz, F.A., Marchesini, N., Seufferheld, M., Govindjee, and Docampo, R., The polyphosphate bodies of Chlamydomonas reinhardtii possess a proton-pumping pyrophosphatase and are similar to acidocalcisomes, J. Biol. Chem., 276, 46196–46203, 2001.
103. Schilde, C., Wassmer, T., Mansfeld, J., Plattner, H., and Kissmehl, R., A multigene family encoding R-SNAREs in the ciliate Paramecium tetraurelia, Traffic, 7, 440–455, 2006.
104. Schmidt-Nielsen, B. and Schrauger, C.R., Amoeba proteus: studying the contractile vacuole by micropuncture, Science, 139, 606–607, 1963.
105. Scott, D.A., Docampo, R., Dvorak, J.A., Shi, S., and Leapman, R.D., In situ compositional analysis of acidocalcisomes in Trypanosoma cruzi, J. Biol. Chem., 272, 28020–28029, 1997.
106. Söllner, T.H., Regulated exocytosis and SNARE function, Mol. Memb. Biol., 20, 209–220, 2003.
107. Steck, T.L., Chiaraviglio, L., and Meredith, S., Osmotic homeostasis in Dictyostelium discoideum: excretion of amino acids and ingested solutes, J. Eukaryot. Microbiol., 44, 503–510, 1997.
108. Stelly, N., Mauger, J.-P., Claret, M., and Adoutte, A., Cortical alveoli of Paramecium: a vast submembranous calcium storage compartment, J. Cell Biol., 113, 103–112, 1991.
109. Stock, C., Allen, R.D., and Naitoh, Y., How external osmolarity affects the activity of the contractile vacuole complex, the cytosolic osmolarity and the water permeability of the plasma membrane in Paramecium multimicronucleatum, J. Exp. Biol., 204, 291–304, 2001.
110. Stock, C., Grønlien, H.K., Allen, R.D., and Naitoh, Y., Osmoregulation in Paramecium: in situ ion gradients permit water to cascade through the cytosol to the contractile vacuole, J. Cell Sci., 115, 2339–2348, 2002.
111. Stock, C., Grønlien, H.K., and Allen, R.D., The ionic composition of the contractile vacuole fluid of Paramecium mirrors ion transport across the plasma membrane, Eur. J. Cell Biol., 81, 505–515, 2002.
112. Stoner, L.C. and Dunham, P.B., Regulation of cellular osmolarity and volume in Tetrahymena, J. Exp. Biol., 53, 391–399, 1970.

113. Sugino, K., Tominaga, T., Allen, R.D., and Naitoh, Y., Electrical properties and fusion dynamics of in vitro membrane vesicles derived from separate parts of the contractile vacuole complex of Paramecium multimicronucleatum, J. Exp. Biol., 208, 3957–3969, 2005.
114. Tani, T., Allen, R.D., and Naitoh, Y., Periodic tension development in the membrane of the in vitro contractile vacuole of Paramecium: modification by bisection, fusion and suction, J. Exp. Biol., 203, 239–251, 2000.
115. Tani, T., Allen, R.D., and Naitoh, Y., Cellular membranes that undergo cyclic changes in tension: direct measurement of force generation by an in vitro contractile vacuole of Paramecium multimicronucleatum, J. Cell Sci., 114, 785–795, 2001.
116. Tani, T., Tominaga, T., Allen, R.D., and Naitoh, Y., Development of periodic tension in the contractile vacuole complex membrane of Paramecium governs its membrane dynamics, Cell Biol. Int., 26, 853–860, 2002.
117. Temesvari, L.A., Rodriquez-Paris, J.M., Bush, J.M., Zhang, L., and Cardelli, J.A., Involvement of the vacuolar proton-translocating ATPase in multiple steps of the endo-lysosomal system and the contractile vacuole system of Dictyostelium discoideum, J. Cell Sci., 109, 1479–1495, 1996.
118. Tominaga, T., Allen, R.D., and Naitoh, Y., Electrophysiology of the in situ contractile vacuole complex of Paramecium reveals its membrane dynamics and electrogenic site during osmoregulatory activity, J. Exp. Biol., 201, 451–460, 1998.
119. Tominaga, T., Allen, R.D., and Naitoh, Y., Cyclic changes in the tension of the contractile vacuole complex membrane control its exocytotic cycle, J. Exp. Biol., 201, 2647–2658, 1998.
120. Tominaga, T., Naitoh, Y., and Allen, R.D., A key function of non-planar membranes and their associated microtubular ribbons in contractile vacuole membrane dynamics is revealed by electrophysiologically controlled fixation of Paramecium. J. Cell Sci., 112, 3733–3745, 1999.
121. Urbina, J.A. and Docampo, R., Specific chemotherapy of Chagas disease: controversies and advance, Trends Parasitol., 19, 495–501, 2003.
122. Vieira, L. L., Lafuente, E., Gamarro, F., and Cabantchik, Z.I., An amino acid channel activated by hypotonically induced swelling of Leishmania major promastigotes, Biochem. J., 319, 691–697, 1996.
123. Vieira, L. L., Lafuente, E., Blum, J., and Cabantchik, Z.I., Modulation of the swelling-activated amino acid channel of Leishmania major promastigotes by protein kinases, Mol. Biochem. Parasitol., 90, 449–461, 1997.
124. Wassmer, T., Froissard, M., Plattner, H., Kissmehl, R., and Cohen, J., The vacuolar proton-ATPase plays a major role in several membrane-bounded organelles in Paramecium, J. Cell Sci., 118, 2813–2825, 2005.
125. Wassmer, T., Kissmehl, R., Cohen, J., and Plattner, H., Seventeen a-subunit isoforms of Paramecium V-ATPase provide high specialization in localization and function, Mol. Biol. Cell, 17, 917–930, 2006.
126. Wessel, D. and Robinson, D.G., Studies on the contractile vacuole of Poterioochromonas malhamensis Peterfi. I. The structure of the alveolate vesicles, Eur. J. Cell Biol., 19, 60–66, 1979.
127. Wistow, G.J., Pisano, M.M., and Chepelinsky, A.B., Tandem sequence repeats in transmembrane channel proteins, Trends Biochem. Sci., 16, 170–171, 1991.
128. Xie, Y., Coukell, M.B., and Gombos, Z., Antisense RNA inhibition of the putative vacuolar $H^+$-ATPase proteolipid of Dictyostelium reduces intracellular $Ca^{2+}$ transport and cell viability, J. Cell Sci., 109, 489–497, 1996.
129. Zeuthen, T., From contractile vacuole to leaky epithelia: coupling between salt and water fluxes in biological membranes, Biochim. Biophys. Acta, 1113, 229–258, 1992.
130. Zhu, Q. and Clarke, M., Association of calmodulin and an unconventional myosin with the contractile vacuole complex of Dictyostelium discoideum, J. Cell Biol., 118, 347–358, 1992.
131. Zhu, Q., Liu, T., and Clarke, M., Calmodulin and the contractile vacuole complex in mitotic cells of Dictyostelium discoideum, J. Cell Sci., 104, 1119–1127, 1993.

# Synaptic Vesicles

**S Takamori**, Tokyo Medical and Dental University, Tokyo, Japan



## Introduction

Communication between neurons or from neurons to their target tissues takes place at a specialized structure called the 'synapse' (Greek meaning 'to clasp'). Synapses consist of two functionally and morphologically distinct components: the presynapse, from which neurotransmitter molecules are released, and the postsynapse, where specific receptors for the respective neurotransmitters are localized on the surface and the complex signaling cascades proceed. As such, one neuron can activate or inactivate connected neurons or target tissues, depending on the transmitter molecule they utilize for their signal transmission. Based on electrophysiological experiments pioneered by Katz and colleagues in the 1960s, it has been postulated that neurotransmitters are released from presynaptic terminals in discrete packets termed 'quanta.' Electron microscopy revealed that at presynaptic terminals, hundreds of small and round membranous vesicles – synaptic vesicles (SVs) – are clustered, which can be reasonably linked to the quanta (**Figure 1**(a)). Furthermore, biochemical experiments using isolated vesicles from mammalian brains have proven that SVs exhibit a variety of transport activities for major chemical transmitters. Based on these findings, it is generally believed that SVs store neurotransmitters and the fusion of SV membrane to the plasma membrane elicits the quantal release of neurotransmitters. Because of their important roles in basic neural functions, much effort has been focused on understanding the molecular machinery of SVs. This article focuses on general features of SVs in terms of morphology, biogenesis, and recycling and their overall molecular composition.

## General Features of Synaptic Vesicles as an Organelle

Clustered at the nerve endings, SVs are one of the most striking morphological hallmarks of presynaptic terminals in electron micrographs. They appear to be roughly homogeneous in size and shape, but it has been determined that some heterogeneity exists among them. Under certain experimental conditions, their shape appeared to be of two types – almost spherical and oval or flat. This difference may be an experimental artifact presumably from the fixation process. Interestingly, this difference in shape may be associated with their transmitter content. It was found that most excitatory, asymmetric glutamatergic synapses contain spherical vesicles, and inhibitory, symmetric, GABAergic synapses contain the latter. Regardless of the functional significance, this observation has provided a possible morphological characteristic to distinguish glutamatergic SVs and GABAergic SVs.

Due to their uniformity in size and abundance in the brain, it is feasible to isolate SVs with high purity and in large amounts – a prerequisite for biochemical and biophysical experiments (**Figure 1**(b)). Electron microscopic observations of isolated SVs from rat brains have revealed that the surface is uneven. They are decorated with one or more prominent globular structures and several spiky or amorphous substructures are observable under electron microscope. After proteolytic digestion these structures are removed and the rims of the lipid bilayer become clearly visible, demonstrating that the vesicles are coated with proteins on the surface (**Figures 1**(c) and **1**(d)). As measured by electron microscopy, their size varies substantially: The diameter of the outer bilayer ranges from 35 to 50 nm, with an average peak at 42 nm. The total dry mass of an average SV was deduced from a combination of protein quantitation, lipid quantitation, and SV particle counting, resulting in approximately 30 attograms (ag) per vesicle, which consists of 17 ag of proteins and 12 ag of lipids. Assuming the thickness of a lipid bilayer is 4 nm, the average inner volume can be estimated as approximately $20 \times 10^{-21}$ l, which provides enough space for approximately 1800 transmitter molecules at a concentration of 150 mM. Within these physical and molecular constraints, SVs are effectively equipped with a unique set of proteins and lipids necessary for executing the fundamental tasks in neurotransmitter release.

## Biogenesis of Synaptic Vesicles

Like other proteins of the secretory pathway, most SV proteins are synthesized at the endoplasmic reticulum and processed through the Golgi apparatus for maturation in the cell body of neurons (**Figure 2**(a)). Conceptually, subdomains which selectively collect the SV proteins bud off from the Golgi apparatus and then travel along the axon to the presynaptic terminals. However, since no vesicles are as small as mature SVs, and some larger nonuniform tubulovesicular structures are seen in the axons, SV constituents are thought to travel along the processes on heterogeneous membranes termed SV precursors.

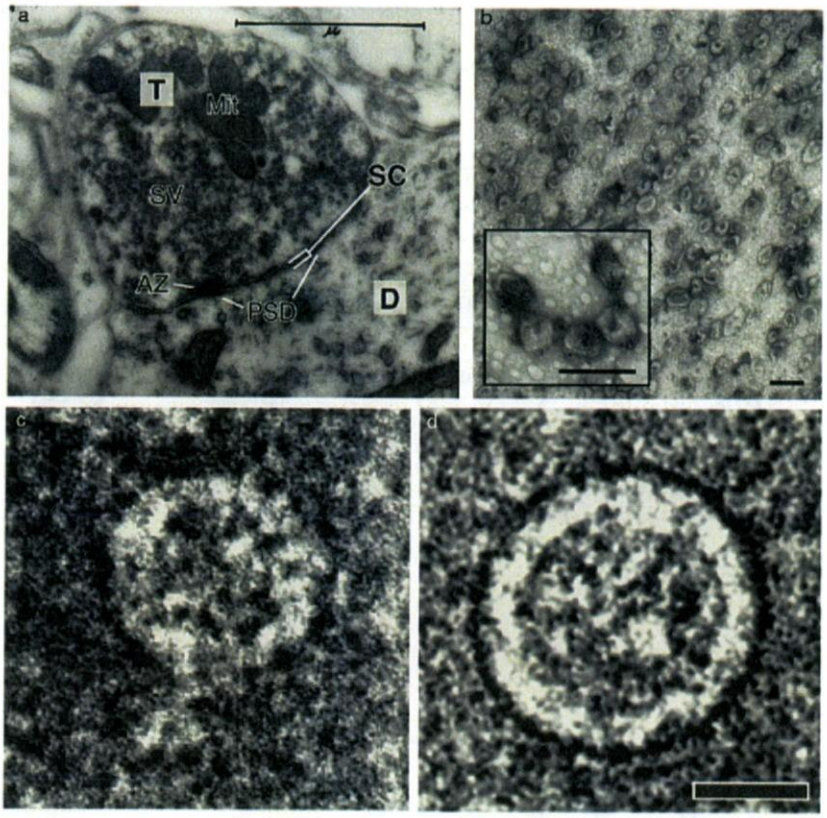


**Figure 1** Morphology of synapse and synaptic vesicles. (a) A transmission electron micrograph of synapse. The presynaptic terminal (T) contains numerous synaptic vesicles (SVs) and mitochondria (Mit). A small portion of SVs is attached to electron dense structures at the presynaptic plasma membrane termed the active zone (AZ), where exocytosis of SVs takes place. Opposite the AZ, there are electron dense structures beneath the postsynaptic membrane termed postsynaptic density (PSD), where neurotransmitter receptors form signaling complexes. D, dendrite; SC, synaptic cleft. (b) An electron micrograph of synaptic vesicle fraction. SVs were purified from mouse whole brains, negatively stained, and imaged by transmission electron microscopy. Inset shows immunogold labeling of the vesicles with an antibody against an SV marker protein, synaptophysin. Approximately 95% of the membranous structures are labeled. (c, d) SVs before (c) and after (d) proteolysis imaged by cryo-electron microscopy. Scale bar = 1 μm (a), 100 nm (b, inset), 20 nm (c). (a) Adapted from the George E. Palade EM Slide Collection at Yale University School of Medicine. (c, d) Reproduced from Takamori S, Holt M, Stenius K, et al. (2006) Molecular anatomy of a trafficking organelle. *Cell* 127: 831–846, with permission from Elsevier.

Once formed, the SV precursor needs a pathway to reach its destination. Microtubules are known to serve as the roads for transporting cargo. Motor proteins of the kinesin superfamily (KIFs) bind to both the microtubules and the cargo, and they control the directional transport of intracellular transporting cargo. Among the KIFs, KIF1A and KIF1B$\beta$ are known to participate in axonal transport of SV precursors. Gene disruption of either KIF1A or KIF1B$\beta$ results in reduction of SV density at the presynaptic terminals and therefore impaired neurotransmission.

The KIF1A- and KIF1B$\beta$-carrying SV precursors contain the major SV marker proteins, such as synaptophysin, synaptobrevin, synaptotagmin, and rab3A, but not presynaptic plasma membrane proteins, such as syntaxin 1 and SNAP-25. In addition, proteins that form the cytomatrix at the active zone, such as piccolo and bassoon, are transported to the axon on distinct cargo, suggesting that segregation of the presynaptic proteins is initiated before they arrive at the terminals. The mechanism by which the SV constituents are selectively recruited into the SV precursor is unknown. It is possible that SV proteins have a specific signal sequence that is assembled and forms microdomains at the exit of the *trans*-Golgi network, but no such common signal sequence has been found. Furthermore, the molecular mechanism regarding how the constituents of the SV precursors can be recognized by KIF1A/1B$\beta$ proteins is poorly understood.

When SV precursors arrive at the presynaptic terminal, they fuse with the plasma membrane where the main route for SV biogenesis is initiated. This route, the AP-2-dependent pathway, is mediated by several essential proteins for vesicle endocytosis, namely clathrin, dynamin, and AP-2. An alternative route by

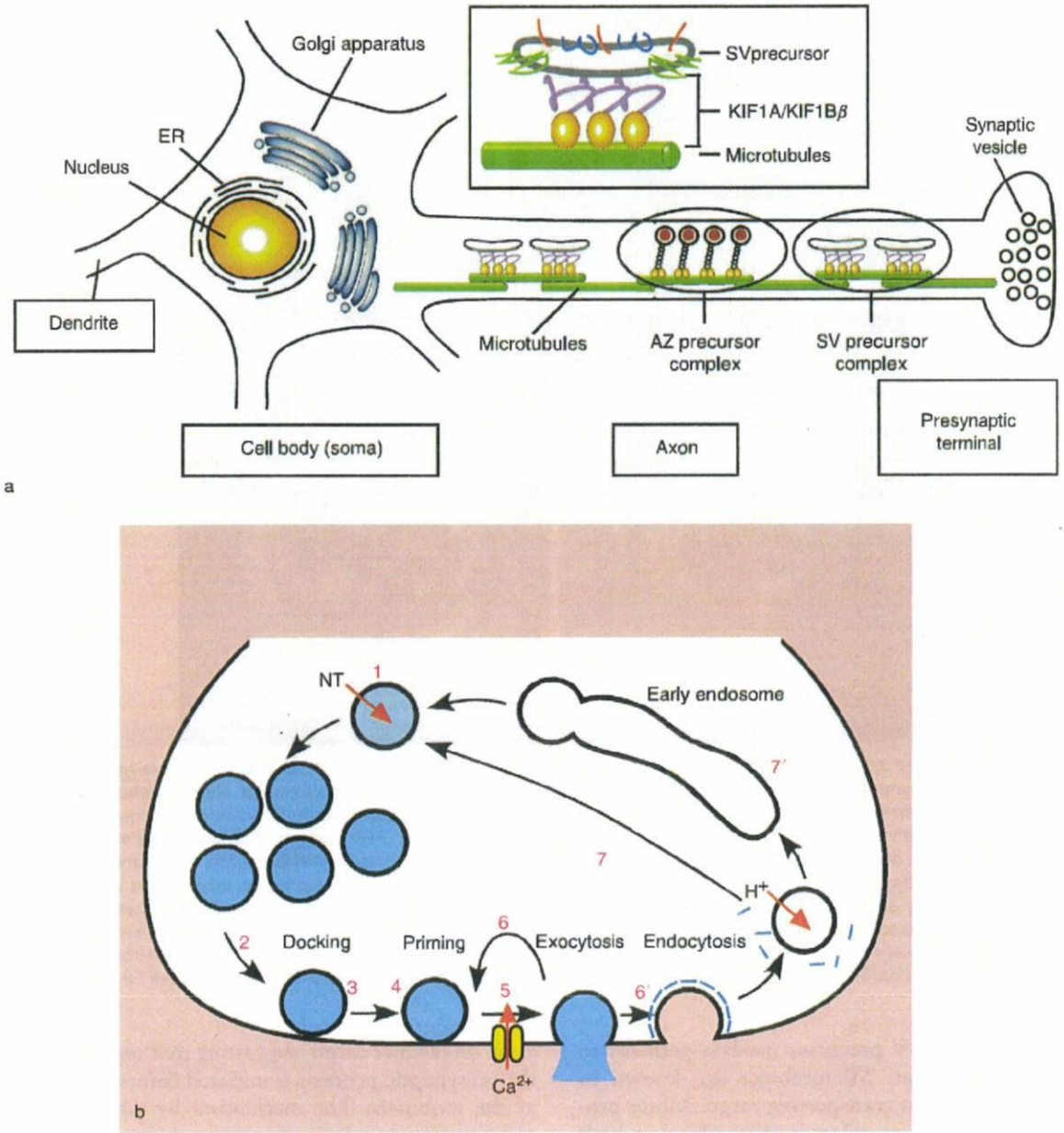


**Figure 2** Biosynthesis and recycling of SVs. (a) Biosynthesis of SVs. SV proteins are synthesized in the cell body of neurons and the SV precursors bud off from the *trans*-Golgi network. The SV precursors are transported along the axon, guided by the microtubules and kinesin motor proteins (KIF1A and KIF1Bβ). (b) SV cycle at presynaptic terminal. (1) SVs are filled with neurotransmitter. (2) The SVs are then transported to the active zone and docked to the presynaptic plasma membrane (docking) (3). The docked SVs become fusion competent by molecular events called priming (4). When an action potential arrives at the terminal, calcium influx through voltage-dependent calcium channels triggers fusion of SV membrane with the plasma membrane (exocytosis), causing discharge of SV content (5). Exocytosed SVs are regenerated either by clathrin-independent fast endocytosis (6) or by clathrin-dependent slow endocytosis (6′). The newly regenerated SVs are immediately refilled with neurotransmitters (7) or, in some case, they undergo fusion steps with early endosomes (7′).

which SVs are generated from early endosomal membranes at the presynaptic terminal is dependent on AP-3. The latter pathway does not seem to account for the majority of SVs since there are no remarkable alterations in SV morphology and numbers in the *mocha* mouse, which lacks functional AP-3. How, then, can SV proteins, but not plasma membrane residents, be recruited into newly generated SVs? Several amino acid sequence motifs or molecular determinants for each SV protein have been proposed to

explain this mechanism. First, a dileucine motif located in the cytoplasmic tails of vesicular transporters (VMAT2, VAChT, and VGLUT1) is important for precise sorting and fast recruitment of those SV proteins. A VAChT mutant which lacks the dileucine motif was trapped at the plasma membrane of the cell body of the differentiated cholinergic SN56 cell lines, and the targeting of the mutant protein to neurites and varicosities (which resemble axon terminals) was dramatically reduced, indicating that the SV precursor cargo carrying VAChT is not directly transported through the axon but is delivered to the plasma membrane of the cell body before being transported along the axon. Second, the intravesicular N-glycosylation of synaptotagmin 1 is essential for its vesicular targeting. Interestingly, synaptotagmin 7, one of the synaptotagmin family members which resides preferentially on the plasma membrane, is targeted to vesicles when the intravesicular portion is replaced with a portion containing the N-glycosylation site of synaptotagmin 1. The mechanistic basis and involvement of other factors is not clear, but the interaction of glycoresidues of synaptotagmin 1 with other proteins at the cell surface may govern the targeting of synaptotagmin 1 to vesicles.

It is likely that multiple factors, including protein–protein interactions and glycoresidue–protein interactions, modulate the sorting of SV proteins. The general principle of the segregation of SV proteins from plasma membrane proteins during SV biosynthesis has not been clarified.

## The Synaptic Vesicle Cycle

At the presynaptic terminals, SVs are not of 'single use.' They are regenerated at the terminals independent from protein synthesis in the cell body. The SV cycle can be outlined, with the uptake of neurotransmitter into SVs as a first step (**Figure 2(b)**, step 1). Neurotransmitters in the central nervous system (CNS) are synthesized locally in the cytoplasm of the presynaptic terminals and are actively transported into SVs. Away from the plasma membrane, the majority of neurotransmitter-filled SVs are either diffusively floating in the cytoplasm or tethered with cytoskeleton components such as actin and spectrin (step 2). For exocytosis, SVs must come into physical contact with the plasma membrane (docking; step 3). SVs do not evenly dock to the whole area of the presynaptic plasma membrane but, rather, to a restricted area called the active zone. There, large cytomatrix proteins, such as bassoon, piccolo, and munc13, form huge protein complexes that appear as electron-dense structures on electron micrographs. Docked SVs are then transformed into fusion-competent SVs via a process called priming (step 4). As soon as an electrical stimulus arrives at the terminal, voltage-dependent calcium channels at the active zone open, resulting in a rapid and local increase in $Ca^{2+}$ concentration. $Ca^{2+}$ ions trigger the fusion of the SV membrane with the plasma membrane in less than 100 μs. Since other exocytotic reactions (i.e., hormone secretion from endocrine cells) take much longer (seconds to minutes), there must be unique factors present only in neurons to perform such a rapid membrane fusion reaction.

After exocytosis, SV components that are incorporated into the plasma membrane are retrieved to form a new SV by endocytosis. There are at least two kinetically distinct modes of endocytosis. The time constants of the fast and slow phase are approximately 1 and 10 s, respectively. Whereas the molecular machinery for the fast phase is not well understood, the slow phase is mediated by the formation of clathrin-coated pits. In both modes, GTP hydrolysis by the GTPase protein dynamin is indispensable for the fission of the invaginated membranes of newly formed SVs. Although various endocytosis-related proteins, such as AP-2, endophilin, amphiphysin, and synaptojanin, have been identified and implicated in controlling endocytosis, their precise roles are a matter of intense research.

The reformed SVs then either recycle back and are refilled with neurotransmitters (step 1) or pass through the early endosomal intermediates before recycling back to step 1. An alternative pathway has been proposed that is similar to the exocytosis of secretory granules; that is, SVs do not fully collapse with the plasma membrane upon fusion but instead form a narrow and transient fusion pore which does not allow a complete discharge of neurotransmitter content. As soon as the pore closes, the half-empty SV can either be immediately engaged in another round of exocytosis or go back to step 1. The existence of such a rapid recycling mode in the CNS, termed the 'kiss-and-run' mechanism, is under debate.

The SVs clustering at the presynaptic terminals can be divided into two functional pools. The first pool contains a small fraction of SVs (5–10% of the total SVs at the presynaptic terminals) that can be released rapidly by a brief high-frequency train of action potentials or by stimulation with hypertonic solution. This pool is thought to be release-ready and is therefore referred as to the readily releasable pool (RRP). The second pool, the reserve pool (RP), represents a vesicle fraction that does not immediate participate in exocytosis. Instead of participating in exocytosis, the RP vesicles replenish the RRP pool after the RRP vesicles undergo exocytosis. Both the amount of the RRP and the rate of replenishment of RRP with RP are critical parameters to determine the availability of vesicles for exocytosis, thereby affecting the

characteristics of short- and long-term plasticity of a given neuron. Classically, the RRP was related to a fraction of morphologically docked vesicles at the plasma membrane and the RP was thought to be spatially distant from the plasma membrane. However, one study suggested that the RRP vesicles do not necessarily correlate with the morphologically docked vesicles but are randomly distributed in the SV cluster at the terminal, indicating that there are no correlations between the anatomical locations of SVs and their functional fusion competence. Mechanisms underlying how the mobility and the fate of an individual SV can be molecularly defined are uncertain.

## Molecular Composition of Synaptic Vesicles

With respect to SV functions as described previously, SVs should be equipped with two classes of essential protein components: transport proteins involved in neurotransmitter uptake into SVs and membrane trafficking proteins involved in the regulation of vesicle cycle and exo-endocytosis. A large body of work has focused on identifying protein components on SVs, leading to an almost complete identification of SV proteins. The stoichiometry of SV proteins may be flexible because many cytoplasmic proteins are temporarily attached to and detached from SVs depending on the status of a specific SV during recycling. On the other hand, a basic set of essential proteins must be present on all SVs for vesicle functions, and the numbers of individual proteins and the proportions within an SV might proteins within an SV to be maintained (**Figure** 3(a)). Furthermore, immunohistochemical studies on SV proteins have demonstrated that most of the major SV proteins consist of multiple isoforms whose expressions in the CNS are partially overlapping or mutually segregated, the combinations of which would create heterogeneity in protein composition in each SV. In contrast to the identification of SV proteins which became relatively handy with advancements in mass spectroscopy, understanding the mechanistic function(s) of each protein has been not so trivial, mainly because of technical limitations with regard to manipulating and measuring the intracellular events with high temporal and spatial resolution. The following sections introduce some of the essential and abundant SV proteins, which are stoichiometric components with at least one copy per SV.

### Proteins for Neurotransmitter Uptake

The accumulation of neurotransmitters in SVs is driven by a proton electrochemical gradient which is generated by a vacuolar-type proton ATPase. The proton pump consists of at least 13 subunits and is the largest functional protein complex in the SV membrane. It contains two functional units – a larger peripheral protein complex ($V_1$) which catalyzes ATP hydrolysis and an integral membrane protein complex ($V_o$) which builds up a ring structure in the membrane and mediates proton translocation. The molecular weight of the entire complex is approximately 800 kDa; therefore, a single complex accounts for approximately 10% of the total SV protein. An SV contains a single copy of the proton pump complex, which may be sufficient to energize neurotransmitter uptake into the SVs.

With the aid of a proton electrochemical gradient, vesicular transporters specific for neurotransmitter-type mediate neurotransmitter uptake into the vesicles. There are four distinct uptake systems for neurotransmitters in the CNS. Three isoforms of vesicular glutamate transporters (VGLUT1–3) transport glutamate into SVs. GABA and glycine share the same transporter, the vesicular inhibitory amino acid transporter (VIAAT; initially called vesicular GABA transporter (VGAT)). Two monoamine transporters (VMAT1 and VMAT2) transport all biogenic amines, with VMAT2 preferentially expressed in the brain. The uptake of acetylcholine is mediated by the vesicular acetylcholine transporter VAChT. All four transporter families belong to the solute carrier protein family, but there are no sequence homologies among the transporters for different neurotransmitter types. There are differences in energetics of the transport; some of them preferentially utilize the membrane potential (VGLUTs) and others use the pH gradient (VMATs and VAChT) as the main driving force. The expression of a particular transporter in the SV membrane is the ultimate determinant for the type of neurotransmitter which is released from a given neuron. Moreover, there are indications that the expression level of the transporter per SV modulates the amount of neurotransmitters accumulated in an SV, thereby regulating quantal size.

In addition to the neurotransmitter transporters discussed previously, SVs contain a chloride channel to facilitate the acidification of SVs. The voltage-dependent chloride channel ClC-3 was proposed to confer this activity on SVs. Although several channel activities, such as a cation selective channel, have been demonstrated by electrophysiological methods on reconstituted systems, the molecular identities of the activities have been elusive. The SV2 protein family and tetraspan vesicle membrane proteins (synaptophysin, synaptogyrin, and SCAMPs) have been identified as SV-specific proteins, and their predicted protein structures suggest their role as a transporter or a channel.

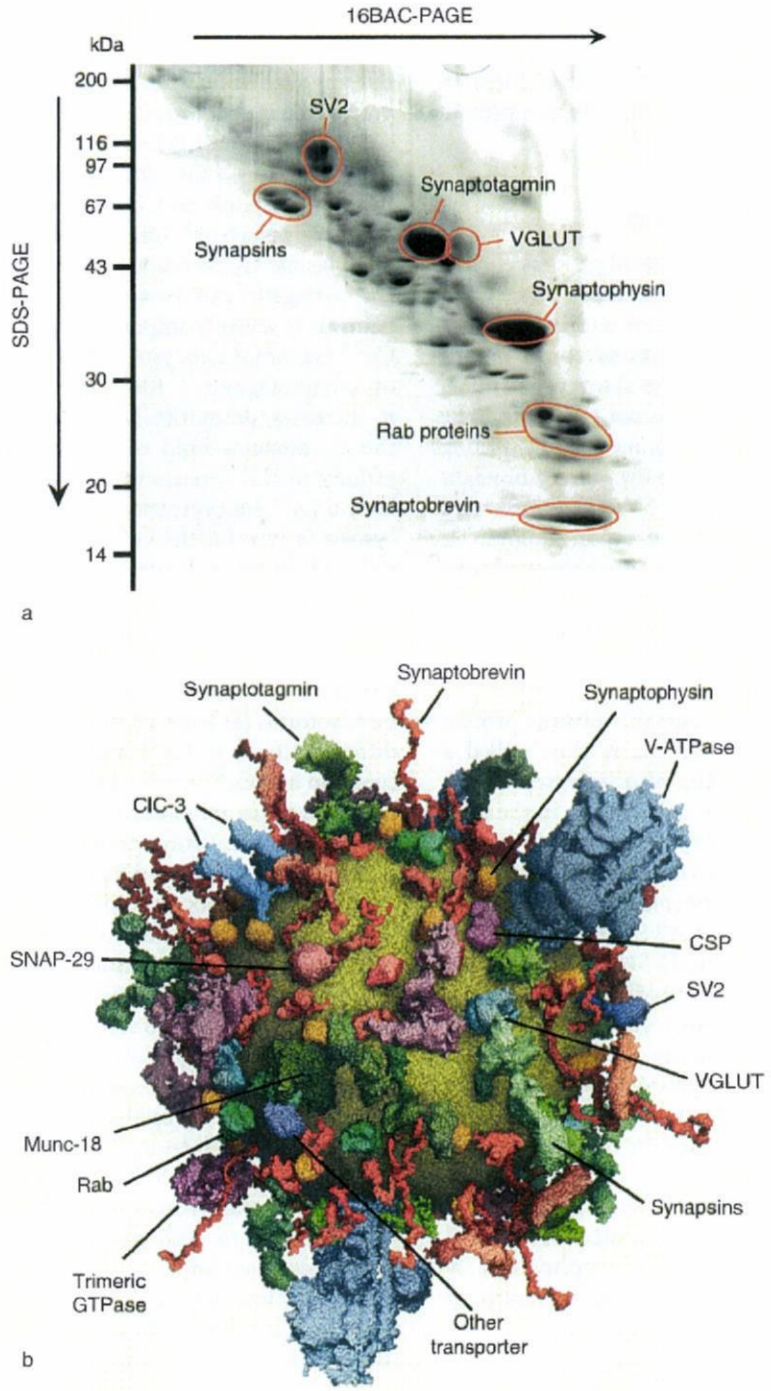


**Figure 3** Molecular composition of SV. (a) Protein composition of SVs visualized by 16-BAC/SDS two-dimensional gel electrophoresis. A total of 500 μg of SV proteins was applied. The spots containing the major SV proteins are circled. (b) Structural model of an average SV. Based on quantitative measurements, a three-dimensional model of an average SV was constructed. An average SV contains 70 copies of synaptobrevin, 30 copies of synaptophysin, 10 copies of neurotransmitter transporter (VGLUT), 8 copies of synapsin, 15 copies of synaptotagmin, 25 copies of Rab GTPase, and 1 or 2 copies of SV2, synaptogyrin, SCAMP, and V-ATPase. The numbers of phospholipids and cholesterol are estimated to be approximately 7000 and 6000, respectively.